Int. J. Heat Mass Transfer. Vol. 36, No. 3, pp. 633–643, 1993
Printed in Great Britain

0017-9310/93 $6.00 + 0.00

Heat and mass transfer in a two-dimensional cross-flow regenerator with a solid conduction effect

JUNG-YANG SAN
Department of Mechanical Engineering, National Chung-Hsing University, 250 KuoKuang Road, Taichung, Taiwan 400, Republic of China

(*Received* 10 *April* 1991 *and in final form* 25 *March* 1992)

Abstract—An analysis of a two-dimensional cross-flow heat and mass regenerator with conductive heat transfer is presented. The adsorbent is a regular density silica gel. Non-switched and switched operations are considered. An enthalpy effectiveness factor is used to specify the regenerator performance. Eight coupled non-linear partial differential equations specify the process of heat and mass transfer. The equations are solved using a finite difference method. The average Lewis number and C_{min}/C_{max} are assumed to be unity. The effects of Ntu, C_r/C_{min}, desiccant content, Biot number and outdoor climate condition on the regenerator performance are analyzed. Both parallel-cross-flow and counter-cross-flow arrangements for sorption are considered. The performance of an ideal regenerator with infinite Ntu and an isothermal wall is analyzed.

1. INTRODUCTION

MUCH RESEARCH on the analysis of solid desiccant dehumidifiers has been performed in recent years [1–15]. However, most of these works are concerned with the adiabatic dehumidification process in rotary dehumidifiers. In this paper a two-dimensional cross-flow heat and mass regenerator is introduced (Fig. 1). Both sides of the regenerator contain silica gel as the adsorbent. The effect of longitudinal heat conduction due to the solid partitions in the regenerator is investigated. The main purpose of this work attempts to determine the best base material for the regenerator.

The idea of using solid desiccant for dehumidification and cooling was originally proposed by Dunkle [1] in the mid 1960s. A brief review of related research works is summarized in the following paragraph.

Maclaine-cross *et al.* [2–5] developed a linear analogy method for predicting the exit fluid temperature and the exit fluid humidity of a desiccant wheel. As compared with the finite difference method, the linear analogy method consumes less computational time. In order to improve the accuracy of the solution, Banks [6, 7] modified the linear analogy method by counting the non-linear effect due to temperature. Comparison with the linear solution showed that his result provided a better match with the finite difference solution. Jurinak [8] applied the above methods to simulate the performance of a desiccant cooling system. A comparison of several numerical solutions was presented in his work. Van den Bulck *et al.* [9] also performed an analysis for a desiccant cooling system. For a given cooling load the optimum regenerative air mass flow rate and the optimum wheel rotational speed were found. The result was plotted in a map as a function of several operating conditions. Van den Bulck *et al.* [10, 11] introduced a theory to simulate the process of heat and mass transfer in a rotary desiccant wheel with infinite transfer coefficients. Combining this with the solution of finite transfer coefficients, the analysis establishes the effectiveness correlation of the desiccant wheel. Klein *et al.* [12] continued the above works. It was found that the enthalpy effectiveness remains the same if the value of C_r/C_{min} reaches a certain limit. Standard techniques for analyzing the single-blow test of sorption process were even less developed. Recently a test procedure for estimating the overall heat and mass transfer coefficients of compact dehumidifier matrices was proposed by Van den Bulck and Klein [13]. The analysis in the test procedure considers the non-linear character of the conservation equations. In the work a comparison between several experimental tests and theoretical analyses was performed.

Pesaran and Mills [14, 15] studied the moisture transport in a packed-bed system. The experimental data have been compared with two analytical results. One is obtained using a solid-side model and the other using a pseudo-gas-side controlled model. From the comparison the former shows a better agreement with the experimental data.

Besides the packed-bed system and the rotary-wheel system, a cross-cooled parallel-plate system was built by Worek and Lavan [16]. The system was tested in a laboratory and a theoretical model for analyzing the system performance was developed by Mathiprakasam and Lavan [17].

In this work switched operation and non-switched operation analyses of the two-dimensional cross-flow

NOMENCLATURE

a, b, c, d, z see Table 1
Bi Biot number, hl_c/k_s
C_{min} minimum flow capacity rate, $[\dot{m}(\partial i_i/\partial T_i)]_{min}$
C_{max} maximum flow capacity rate, $C_{max} = C_{min}$
C_r regenerator capacity rate, $m_w C_{wr}/t_{BF}$
C_w specific heat of wet desiccant material [kJ kg K^{-1}]
C_{wr} reference specific heat, 1.0 kJ kg^{-1} K^{-1}
D_h hydraulic diameter [m]
f desiccant content [g desiccant (g total weight)$^{-1}$]
h convective heat transfer coefficient [kW m^{-2} K^{-1}]
h_{fg} heat of evaporation [kJ kg^{-1}]
H height of regenerator [m]
i specific enthalpy of moist air [kJ kg^{-1}]
$\bar{i}$ average specific enthalpy [kJ kg^{-1}]
k_s overall thermal conductivity of solid [W m^{-1} K^{-1}]
k_y convective mass transfer coefficient [kg m^{-2} s^{-1}]
k_1 thermal conductivity of air [W m^{-1} K^{-1}]
k_2 thermal conductivity of plate material [W m^{-1} K^{-1}]
k_3 average thermal conductivity of desiccant material [W m^{-1} K^{-1}]
l_1 channel spacing [mm]
l_2 plate thickness [mm]
l_3 thickness of desiccant material [mm]
l_e effective heat transfer length [mm]
L channel length or width [m]
Le average Lewis number, $h/[k_y(\partial i_i/\partial T_i)]$
$\dot{m}$ total air mass flow rate on one side [kg s^{-1}]
m_w mass of desiccant material on one side
n number of channels on one side
Ntu number of transfer unit, $nhx_{1F}x_{2F}/\dot{m}(\partial i_i/\partial T_i)$
P_w vapor pressure on desiccant surface [atm]
P_{ws} saturation vapor pressure [atm]
Q heat of adsorption [kJ (kg H_2O)$^{-1}$]
RH relative humidity × 100, $P_w/P_{ws} \times 100$
t non-dimensional time, $\dot{m}(\partial i_i/\partial T_i)/(m_w C_{wr}/t_B)$
t_A time [s]
t_B reduced time, $t_A - x_1/u$ [s]
t_{AF} mode operating period [s]
t_{BF} total reduced time, $t_{AF} - x_1/u$ [s]
T fluid temperature [°C]
$\bar{T}$ average fluid temperature [°C]
T_w desiccant surface temperature [°C]
u fluid velocity [m s^{-1}]
V_d volume of desiccant material [m^3]
W moisture content [kg H_2O (kg desiccant)$^{-1}$]
x_1, x_2, x_3 coordinate notations
X_1 non-dimensional x_1 coordinate, x_1/x_{1F}
X_2 non-dimensional x_2 coordinate, x_2/x_{2F}
x_{1F} channel length [m]
x_{2F} channel width [m]
Y humidity ratio [kg H_2O (kg air)$^{-1}$]
$\bar{Y}$ average humidity ratio [kg H_2O (kg air)$^{-1}$]
Y_w humidity ratio on desiccant surface [kg H_2O (kg air)$^{-1}$].

Greek symbols
$\gamma_{1,i}$ $C_{wr}/[fLe(\partial i_i/\partial T_i)]$
$\gamma_{2,i}$ $C_{w,i}/C_{wr}$
$\gamma_{3,i}$ $Q_i/[Le(\partial i_i/\partial T_i)]$
ε_H enthalpy effectiveness
ρ_d density of desiccant material [kg m^{-3}].

Subscripts
a adsorption stream
d desorption stream
e exit state
i inlet state or stream
j stream.

heat and mass regenerator are performed. In practical applications the regenerator is designed with the switched operation. In the switched operation the heat and mass regenerator can be used as a ventilator in conventional air conditioning systems. In doing so, an exchange of enthalpy between the outdoor air and the exhaust room air results. Thus the air conditioner can be operated in a complete recirculation mode and the latent load can be reduced. The present work deals with the general characteristics of the heat and mass regenerator. The effects of C_r/C_{min}, Ntu, desiccant content, Biot number and outdoor climate condition on the performance of the regenerator are individually discussed.

2. MATHEMATICAL MODEL

The mathematical model for analyzing the heat and mass transfer in the two-dimensional cross-flow regenerator is developed. The geometry of the two-dimensional channel is shown in Fig. 2, in which the solid plate serves as a partition for the two neighboring flows. The desiccant material is coated on both sides of the channel and it is composed of a regular density silica gel and a substratum. The substratum is made of glass fiber or mylar tape and the solid plate can be an aluminum sheet. The isotherms and the heat of adsorption of the silica gel are listed in Table 1 [8]. The major assumptions in the mathematical model are summarized as follows:

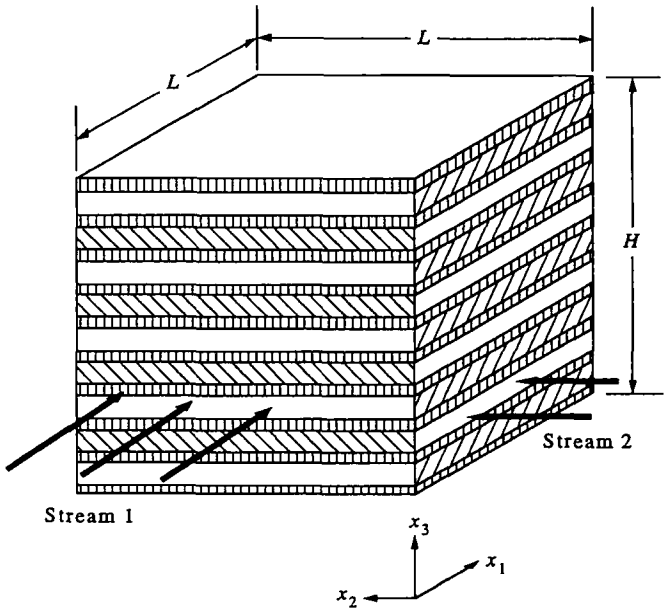

FIG. 1. Schematic of a two-dimensional cross-flow heat and mass regenerator.

(i) The axial heat and mass diffusion in the air streams are neglected.

(ii) The flow capacity rates of the dry stream and the humid stream are balanced ($C_{max} = C_{min}$) and the convective heat transfer coefficients are the same for the two streams.

(iii) The flow length and the channel spacing are the same on both sides of the regenerator.

(iv) The solid element (desiccant material) is treated as a lumped capacitance which exchanges heat and mass only with its neighboring fluid element.

(v) A pseudo-steady-state operation is assumed for the heat transfer in the solid plate. The conductive heat transfer between the adsorption side and the desorption side is considered to be one-dimensional. A characteristic length, l_c, is used to express the overall conductive heat transfer length.

Based on the above assumptions the eight governing equations for the heat and mass transfer in the regenerator can be expressed as follows:

(i) mass balance for fluid element

$$\left(\frac{\dot{m}}{nx_{jF}}\right)\left[\left(\frac{\partial Y_i}{\partial x_i}\right)_{t_A} + \frac{1}{u}\left(\frac{\partial Y_i}{\partial t_A}\right)_{x_i}\right] = 2k_y(Y_{w,i} - Y_i) \quad (1)$$

(ii) mass balance for solid element

$$\left(\frac{fm_w}{nx_{1F}x_{2F}}\right)\left(\frac{\partial W_i}{\partial t_A}\right)_{x_i} = 2k_y(Y_i - Y_{w,i}) \quad (2)$$

(iii) energy balance for fluid element

$$\frac{\dot{m}(\partial i_i/\partial T_i)}{nx_{jF}}\left[\left(\frac{\partial T_i}{\partial x_i}\right)_{t_A} + \frac{1}{u}\left(\frac{\partial T_i}{\partial t_A}\right)_{x_i}\right] = 2h(T_{w,i} - T_i) \quad (3)$$

(iv) energy balance for solid element

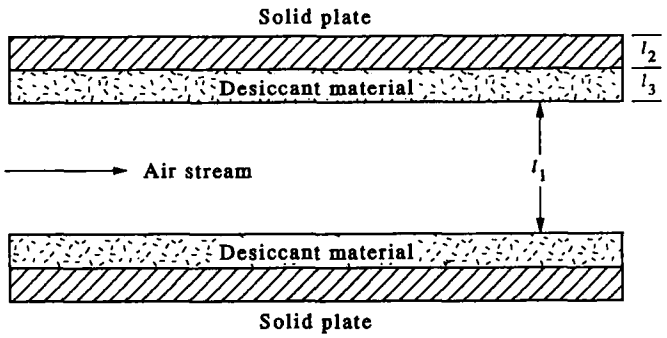

FIG. 2. Schematic of a two-dimensional channel flow.

Table 1. Silica gel properties

Heat of adsorption

$$Q = h_{fg}(1.0+0.2843\exp(-10.28W))$$

Equilibrium isotherm

$$RH/100 = (2.112W)^{Q/h_{fg}}(29.91P_{ws})^{(Q/h_{fg}-1)}$$

Saturation pressure (atm)

$$\log_{10}\frac{P_{ws}}{218.167} = -\left(\frac{z}{T+273.15}\right)\left(\frac{a+bz+cz^3}{1+dz}\right)$$

where

$$z = 374.12-T$$
$$a = 3.2437814$$
$$b = 5.86826\,(10)^{-3}$$
$$c = 1.1702379\,(10)^{-8}$$
$$d = 2.1878462\,(10)^{-3}$$

ASHRAE data

$$Y_w = \frac{0.622\,RH}{10^{4.21429-(7.5T_w/(237.3+T_w))}-RH}$$

$$\left(\frac{C_{w,i}m_w}{nx_{1F}x_{2F}}\right)\left(\frac{\partial T_{w,i}}{\partial t_A}\right)_{x_i} = 2h(T_i-T_{w,i}) + 2\left(\frac{k_s}{l_c}\right)(T_{w,j}-T_{w,i}) + 2Q_ik_y(Y_i-Y_{w,i}) \quad (4)$$

where $i, j = 1$ or 2, but $i \neq j$.

In equation (4) one-dimensional conductive heat transfer between the adsorption side and the desorption side is assumed. The conductive heat transfer rate is expressed as follows

$$q'' = (T_{w,j}-T_{w,i})/(l_c/k_s) \quad (5)$$

where

$$l_c/k_s \equiv 2(l_3/k_3)+(l_2/k_2).$$

In the above equation (l_c/k_s) is the overall thermal resistance in the solid. In the case with a metallic plate as the partition the value of (l_2/k_2) will be much smaller than that of (l_3/k_3). If so, (l_2/k_2) can be neglected, thus k_3 will stand for k_s and l_c will be $2l_3$.

For the convenience of analysis a reduced time, t_B, is introduced into equations (1)–(4). The reduced time is defined as $[t_A-(x_i/u)]$. Using the expression of t_B the following relationship can be derived

$$\left(\frac{\partial Y_i}{\partial x_i}\right)_{t_A} + \frac{1}{u}\left(\frac{\partial Y_i}{\partial t_A}\right)_{x_i} = \left(\frac{\partial Y_i}{\partial x_i}\right)_{t_B} \quad (6)$$

$$\left(\frac{\partial W_i}{\partial t_A}\right)_{x_i} = \left(\frac{\partial W_i}{\partial t_B}\right)_{x_i} \quad (7)$$

$$\left(\frac{\partial T_i}{\partial x_i}\right)_{t_A} + \frac{1}{u}\left(\frac{\partial T_i}{\partial t_A}\right)_{x_i} = \left(\frac{\partial T_i}{\partial x_i}\right)_{t_B} \quad (8)$$

$$\left(\frac{\partial T_{w,i}}{\partial t_A}\right)_{x_i} = \left(\frac{\partial T_{w,i}}{\partial t_B}\right)_{x_i}. \quad (9)$$

Substituting equations (6)–(9) into equations (1)–(4), the governing equations for the heat and mass transfer can be simplified as follows

$$\left(\frac{\partial Y_i}{\partial X_i}\right)_{t_i} = 2Ntu(1.0/Le)(Y_{w,i}-Y_i) \quad (10)$$

$$\left(\frac{\partial W_i}{\partial t_i}\right)_{x_i} = 2Ntu\gamma_{1,i}(Y_i-Y_{w,i}) \quad (11)$$

$$\left(\frac{\partial T_i}{\partial X_i}\right)_{t_i} = 2Ntu(T_{w,i}-T_i) \quad (12)$$

$$(\gamma_{2,i}/2Ntu)\left(\frac{\partial T_{w,i}}{\partial t_i}\right)_{x_i} = (T_i-T_{w,i}) + (1.0/Bi)(T_{w,j}-T_{w,i}) + \gamma_{3,i}(Y_i-Y_{w,i}) \quad (13)$$

where $i, j = 1$ or 2, but $i \neq j$.

The above eight governing equations are solved using a numerical method. The numerical method is composed of a forward finite difference scheme and a higher-order backward finite difference scheme. The input parameters of the numerical method are arranged to be Ntu, C_r/C_{min}, f, Bi and indoor and outdoor air temperatures and humidity ratios.

Equations (10)–(13) represent a general form of the governing equations for the heat and mass transfer process in desiccant dehumidification. In the case that Bi is zero, $T_{w,1}$ will be equal to $T_{w,2}$. There will be seven unknowns remaining in the problem. In this case the two equations represented by equation (13) should be added together and the term relating to the conductive heat transfer effect dropped. For the cross-cooled dehumidifier introduced in ref. [17], one side of the dehumidifier is for sorption ($i = 1$) and the other side is for cooling ($i = 2$). In this case there will be no mass diffusion in the cooling channel and thus equations (10) and (11) will only hold for the case with $i = 1$.

In the case that the value of Bi is infinite and subscripts i and j are dropped, the set of equations (10)–(13) represents the four governing equations for the heat and mass transfer process in an adiabatic dehumidifier. A comparison for the case with an infinite Bi between the present approach and those in refs. [4, 5, 8] will be shown later in this work.

2.1. *Limiting operation*

As the value of Ntu is infinitely large, the cross-flow heat and mass regenerator is termed to be operated at its limit. There are two special cases corresponding to the limiting operation. One of the cases is with an adiabatic wall ($Bi = \infty$) and the other is with an isothermal wall ($Bi = 0$). When the wall is adiabatic, the process in the cross-flow regenerator will be the same as that in a rotary-type heat and mass regenerator. The limiting operation of a rotary-type heat and mass regenerator has been analyzed by Van den Bulck *et al.* [10] and Klein *et al.* [12]. Their solutions can be applied to the present case, providing that some proper conversions of the non-dimensional parameters are performed.

For the case with an isothermal wall the governing equations will be as follows

$$Le\left(\frac{\partial Y_{w,1}}{\partial X_1}\right)_t+\frac{1}{\gamma_{1,1}}\left(\frac{\partial W_1}{\partial t}\right)_{x_1}=0 \quad (14)$$

$$Le\left(\frac{\partial Y_{w,2}}{\partial X_2}\right)_t+\frac{1}{\gamma_{1,2}}\left(\frac{\partial W_2}{\partial t}\right)_{x_2}=0 \quad (15)$$

$$(\gamma_{2,1}+\gamma_{2,2})\left(\frac{\partial T_w}{\partial t}\right)=-\left(\frac{\partial T_w}{\partial X_1}\right)_t-\left(\frac{\partial T_w}{\partial X_2}\right)_t$$
$$-\gamma_{3,1}Le\left(\frac{\partial Y_{w,1}}{\partial X_1}\right)_t-\gamma_{3,2}Le\left(\frac{\partial Y_{w,2}}{\partial X_2}\right)_t \quad (16)$$

where

$$W_1=W_1(T_w, Y_{w,1})$$
$$W_2=W_2(T_w, Y_{w,2}).$$

For the limiting operation the transfer equations of the heat and mass are eliminated [10, 12]. The governing equations thus are reduced from the original eight equations to the above three equations. The set of equations is in a wave form. Since it is two-dimensional the traditional method of characteristics is hard to apply to solve for the solution. In this work a forward finite difference scheme is developed. The result of the numerical analysis will be shown later in this paper.

3. EFFECTIVENESS FACTOR

An effectiveness factor, ε_H, is used to specify the periodic steady-state performance of the heat and mass regenerator. This factor is defined as follows

$$\varepsilon_H=\frac{\bar{i}_{a,i}-\bar{i}_{a,e}}{\bar{i}_{a,i}-\bar{i}_{d,i}}. \quad (17)$$

On the right-hand side of the above equation, the numerator is the actual amount of energy transfer in the regenerator and the denominator is the maximum amount possible energy transfer for the two inlet conditions. In equation (17) $\bar{i}$ is the average enthalpy of the moist air. It is evaluated as follows:

$$\bar{i}=1.0046465\bar{T}+\bar{Y}(2467.4203+1.8837122\bar{T}) \quad (18)$$

where $\bar{T}$ and $\bar{Y}$ are, respectively, the time and spatial-averaged temperature and humidity ratios.

4. NON-SWITCHED OPERATION

An analysis for the non-switched operation of the heat and mass regenerator is performed. The nominal outdoor air temperature and humidity ratio (stream 1) are, respectively, 35°C and 0.0142 kg H_2O (kg air)$^{-1}$. The indoor air temperature and humidity ratio (stream 2) are, respectively, 26°C and 0.0112 kg H_2O (kg air)$^{-1}$. The initial temperature of the regenerator is 40 C and the initial water content of the desiccant material is 0.01 kg H_2O (kg silica gel)$^{-1}$. In the analysis the desiccant content is 0.3 and the *Ntu* is 2.5. Three different values of Biot number are considered. The case with a Biot number of infinity indicates an insulated condition between the adsorption stream and the desorption stream; the case with a Biot number of 0.1 represents a high conductive heat transfer rate between the two sides; the case with a Biot number of unity stands for a normal conductive heat transfer rate.

Figure 3 shows the exit air temperature and humidity ratio for stream 1. For the case with a Biot number of infinity, there is no conductive heat transfer between the two streams. After a long operating period the desiccant material will be thermally and dynamically saturated. At this moment, the exit air temperature and humidity ratio will equal the inlet air temperature and humidity ratio. For the case with a Biot number of 0.1, the conductive thermal resistance is almost negligible. After a long operating period the desiccant material will be dynamically saturated and from then onwards the heat and mass regenerator will act as a recuperator. In the considered case the temperature effectiveness approaches 0.65 which is the value normally found in heat exchanger design texts [18]. The case with a Biot number of unity shows an exit air temperature somewhere in between the exit air temperatures for the above two cases. Similarly, after a long operating period the exit air temperature and humidity ratio will individually approach a certain value.

Figure 4 shows the exit air temperature and humidity ratio for stream 2. Similar to the result shown in Fig. 3, after a long operating period the humidity ratio for the three cases approaches the inlet air humidity ratio. As far as the exit air temperature is concerned, it increases as the value of the Biot number decreases. For the case with a Biot number of infinity, there is no conductive heat transfer between the two streams and eventually the exit air temperature equals the inlet air temperature, 26°C.

5. SWITCHED OPERATION

A periodic steady-state analysis for the switched operation is performed in this work. The convergence of the periodic steady-state operation is very slow. From the analysis the larger the *Ntu*, the longer the computational time. Two different flow arrangements are considered in this work. One is termed as a counter-cross-flow arrangement which has a counter-flow arrangement for sorption. The other is termed as a parallel-cross-flow arrangement which has a parallel-flow arrangement for sorption.

5.1. *Effect of Biot number and operating period*

The major difference between the analysis of the cross-flow heat and mass regenerator and the analysis of an adiabatic rotary heat and mass regenerator [8] is due to the direct conductive heat transfer between the two streams. The rate of the conductive heat trans-

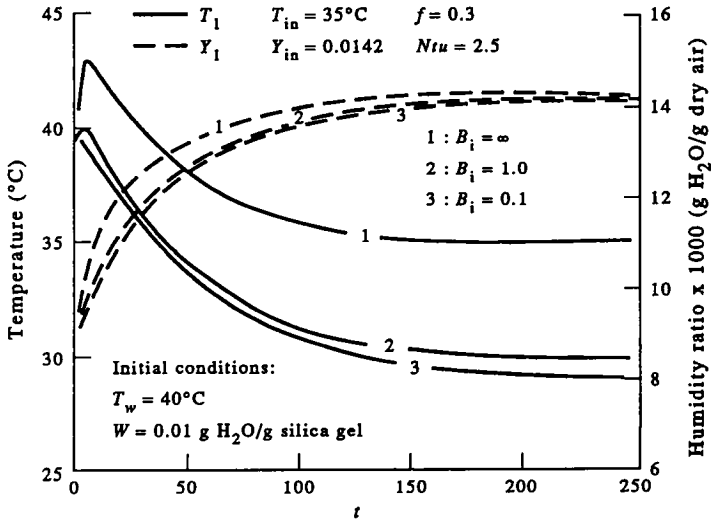

FIG. 3. Exit air temperature and humidity (X_1-direction).

fer mainly depends on the thermal conductivity of the solid. In the case with a large thermal conductivity, heat can be transferred easily from the high temperature side to the low temperature side. In the case with a small thermal conductivity, the heat transfer rate will be very little and thus the process in the cross-flow heat and mass regenerator will be similar to that in an adiabatic rotary heat and mass regenerator. In this section the effect of the conductive heat transfer on the performance of the cross-flow heat and mass regenerator is analyzed.

Figures 5 and 6 show the effect of the Biot number on the effectiveness factor. The nominal indoor temperature and humidity ratio are, respectively, 26°C and 0.0112 kg H_2O (kg air)$^{-1}$. The outdoor temperature and humidity ratio are, respectively, 28°C and 0.0185 kg H_2O (kg air)$^{-1}$.

Figure 5 shows the results for the counter-cross-flow arrangement and Fig. 6 the parallel-cross-flow arrangement. Both Figs. 5 and 6 show that the Biot number significantly affects the enthalpy effectiveness of the regenerator. In the low value range of C_r/C_{min}, the lower the value of Biot number, the higher the enthalpy effectiveness of the regenerator. For the parallel-cross-flow arrangement an optimum value of C_r/C_{min} exists. The optimum C_r/C_{min} corresponds to the maximum enthalpy effectiveness for a set of Ntu, Bi and f. From the analysis it shows that the maximum

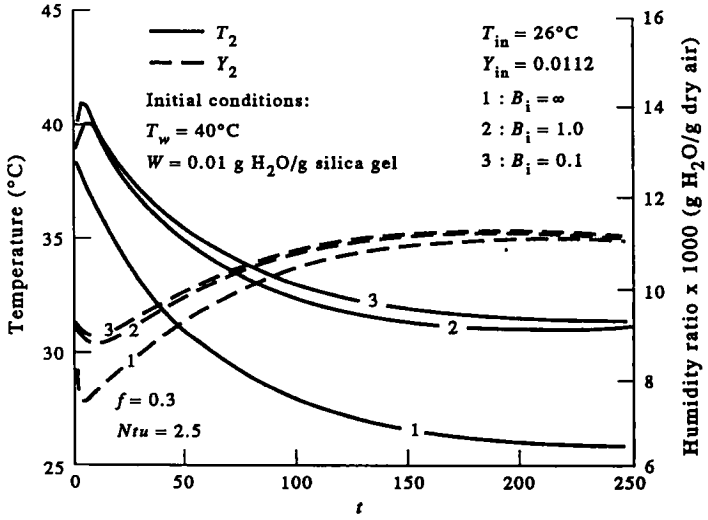

FIG. 4. Exit air temperature and humidity (X_2-direction).

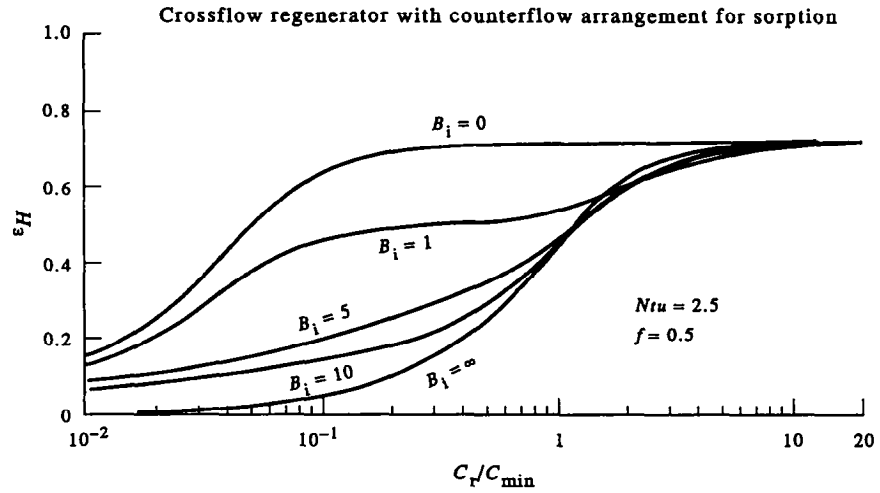

FIG. 5. Effect of operating period and Biot number with counter-cross-flow arrangement.

enthalpy effectiveness reaches a minimum for a value of the Biot number near 2.0.

By varying the value of C_r/C_{min} the enthalpy effectiveness will be altered. Figures 5 and 6 also show the effect of C_r/C_{min} on the effectiveness factor. Figure 5 reveals that the enthalpy effectiveness approaches 0.71 for the value of C_r/C_{min} approaching infinity. Figure 6 shows that the enthalpy effectiveness approaches 0.49 as the value of C_r/C_{min} approaches infinity. This tendency is similar to that for a rotary-heat regenerator. Also it indicates that the performance of a regenerator with the counter-cross-flow arrangement is much better than that of the parallel-cross-flow arrangement.

5.2. *Effect of outdoor climate condition*

Figures 7 and 8 show the effect of the outdoor climate condition on the performance of the regenerator. For convenience of analysis three outdoor conditions are nominated. There are 28°C and 0.0185 kg H_2O (kg air)$^{-1}$ (pt. 2), 30°C and 0.0185 kg H_2O (kg air)$^{-1}$ (pt. 2′), 30°C and 0.015 kg H_2O (kg air)$^{-1}$ (pt. 2″). The result reveals that the enthalpy effectiveness barely depends on the three outdoor climate conditions. Figure 7 also shows an interesting result. For the counter-cross-flow arrangement a point exists which provides the minimum amount of sensible cooling. However it does not represent the point with the minimum enthalpy effectiveness.

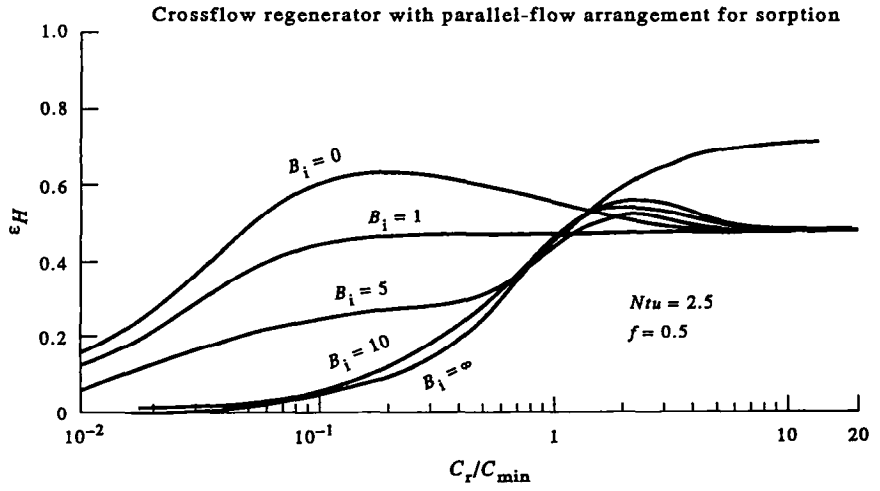

FIG. 6. Effect of operating period and Biot number with parallel-cross-flow arrangement.

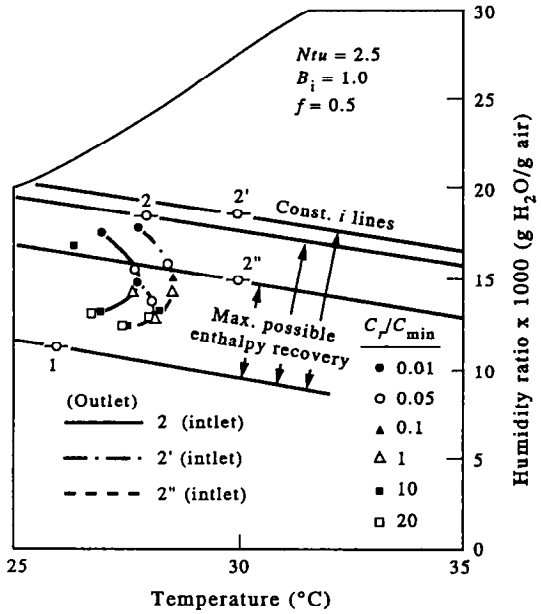

FIG. 7. Outlet states of streams 2, 2′ and 2″ for counter-cross-flow arrangement.

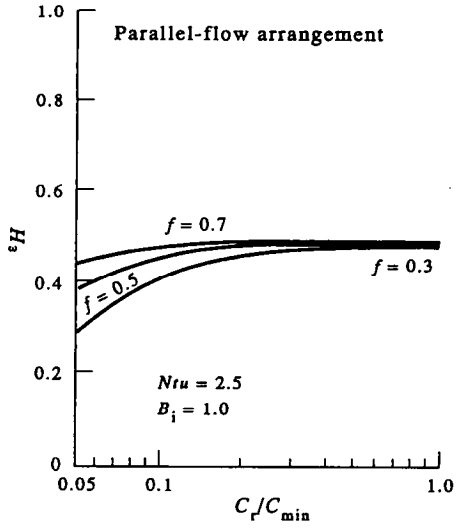

FIG. 9. Effect of desiccant content.

5.3. *Effects of f and Ntu*

Figure 9 shows the enthalpy effectiveness of three heat and mass regenerators for operation with various values of C_r/C_{min} and a parallel-flow arrangement. The three heat and mass regenerators individually have a desiccant content of 0.3, 0.5 and 0.7, but they all have the same Biot number of 1.0. The nominal *Ntu* is 2.5. The result shows that the values of the enthalpy effectiveness for the three cases, at a large value of C_r/C_{min} are very close. Thus the desiccant content has very little influence on the enthalpy effectiveness. The result also shows that, for the same value of C_r/C_{min}, the enthalpy effectiveness increases as the desiccant content increases. Therefore the operating period of a regenerator with a high desiccant content can be longer than that of another regenerator with a low desiccant content.

Figure 10 represents the enthalpy effectiveness for the *Ntu* of 2.5, 3.5, 4.5 and infinity. The result shows that the enthalpy effectiveness increases as the *Ntu* increases. Besides that, the increase of the enthalpy effectiveness tends to be proportional to the increase of *Ntu* for the value of *Ntu* in the range between 2.5 and 4.5. Although the result in Fig. 10 is based on a Biot number of 1.0 and a desiccant content of 0.5, the trend should be valid for various Biot numbers and desiccant contents. For a regenerator with a *Ntu* of infinity and Biot number of zero, the enthalpy effectiveness will approach 1.0 for high C_r/C_{min} operations. A regenerator of this type thus can be considered to be an ideal regenerator.

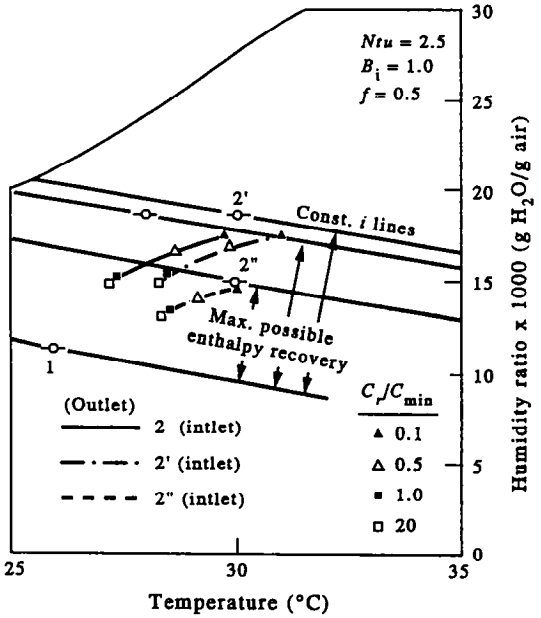

FIG. 8. Outlet states of streams 2, 2′ and 2″ for parallel-cross-flow arrangement.

6. NUMERICAL EXAMPLE

A numerical example illustrating the design of the size and the operating time period of a two-dimensional cross-flow heat and mass regenerator is presented. It is assumed that each side of the regenerator is individually arranged to be a parallel-flow operation during the switch of adsorption and desorption. The heat and mass regenerator is composed of

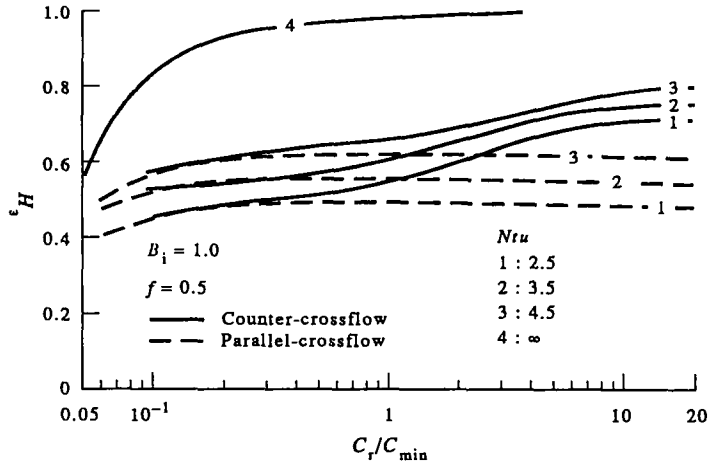

FIG. 10. Effect of *Ntu*.

aluminum sheets and a desiccant material. The aluminum sheet acts as a partition between the two neighboring desiccant materials. The desiccant material contains the same silica gel as considered before and has glass fiber as the substratum. The specifications of the heat and mass regenerator are summarized as follows: $f = 0.3$, $\rho_d = 710$ kg m^{-3}, $l_1 = 2$ mm, $l_{2,3} = 0.2$ mm. The Nusselt number and the thermal conductivity of the air are considered to be constant, respectively, 8.23 and 0.027 W m^{-1} K^{-1}. The convective heat transfer coefficient, h, is calculated using Nu, k_1 and D_h to be 0.0556 kW m^{-2} K^{-1}. The selected Ntu and C_r/C_{min} are, respectively, 4.5 and 0.3. The value of k_s/l_c for this example is evaluated to be 0.022 W m^{-2} K^{-1}, thus the Biot number is 1.0. From the analysis of the switched operation the corresponding enthalpy effectiveness is 0.590.

From the definition of Ntu and C_r/C_{min} the air mass flow rate and the total reduced time, respectively, can be expressed as follows

$$m_w = 0.012 n x_{1F} x_{2F} \tag{19}$$

$$t_{BF} = 3.23 m_w / \dot{m}. \tag{20}$$

If there are 40 channels on one side, the height of the regenerator, H, will be 0.192 m. Furthermore, if the air mass flow rate is specified as 0.043 kg s^{-1}, using equation (19) the product of x_{1F} and x_{2F} can be calculated to be 0.09 m^2. In this example x_{1F} is considered to be the same as x_{2F}. Taking the square root of 0.09, both x_{1F} and x_{2F} will equal 0.3 m. Since the values of x_{1F} and x_{2F} are much greater than the channel spacing, the assumption of two-dimensional fully developed flow is valid.

In equation (20) m_w is a half weight of the desiccant material in the heat and mass regenerator and it can be related to x_{1F}, x_{2F}, n and l_3 in the following form

$$m_w = \rho_d V_d = 2 l_3 n x_{1F} x_{2F} \rho_d. \tag{21}$$

Substituting the values of ρ_d, l_3, n, x_{1F} and x_{2F} into equation (21), m_w is evaluated to be 1.02 kg. Multiplying m_w by a factor of 2.0, the total weight of the desiccant material, 2.04 kg, is obtained. Since the desiccant content is 0.3, the total weight of the silica gel is 0.612 kg. Once m_w is known, using equation (20) t_{BF} will be 76.8 s. The value of t_{BF} usually is very close to the value of the mode operating period. In engineering applications t_{BF} can be considered to be the real mode operating period.

7. ACCURACY OF THE COMPUTER MODEL

If the value of Bi is infinite and subscript i is dropped, equations (10)–(13) become the same as the governing equations for the heat and mass transfer process in an adiabatic rotary dehumidifier. The equations for adiabatic rotary dehumidifier had been solved thoroughly by many other scholars [8], thus the accuracy of the present model can be found by conducting a direct comparison between the solution for a rotary dehumidifier and the solution for a cross-flow heat and mass regenerator with a Bi of infinity. The rotary dehumidifier usually is operated with a counter-flow arrangement, the same flow arrangement for adsorption and desorption during the switched operation thus is considered for the cross-flow regenerator.

Based on the same operating conditions as the three cases in Jurinak's work [8], several computer runs are performed in order to compare the present model with Maclaine-cross and non-linear analogy methods. The results of the comparison are listed in Table 2. Generally speaking, a good agreement between the present

Table 2. Outlet temperature and humidity ratio of the adsorption stream

Operating condition	Present model		Maclaine-cross method		Non-linear analogy method	
	T (°C)	Y (g kg^{-1})	T (°C)	Y (g kg^{-1})	T (°C)	Y (g kg^{-1})
(1) $Ntu = 1.25$ $C_r/C_{min} = 0.5$	57.55	9.66	57.31	9.76	57.97	9.08
(2) $Ntu = 1.25$ $C_r/C_{min} = 0.25$	55.88	9.04	55.78	8.86	56.50	8.05
(3) $Ntu = 5.0$ $C_r/C_{min} = 0.5$	67.54	6.86	66.73	6.75	67.06	6.36

Inlet state of the adsorption stream: 35°C, 14.2 g kg^{-1}.
Inlet state of the desorption stream: 85°C, 14.2 g kg^{-1}, $f = 0.5$.

model and the Maclaine-cross finite difference scheme is observed. As far as the non-linear analogy method is concerned [6, 7], it is a simplified approach for solving hyperbolic-type equations. This method consumes much less computational time than that of the finite difference methods, but it also provides less accuracy.

8. CONCLUSIONS

In the non-switched operation, as the operating time period increases, eventually the process in the heat and mass regenerator will be similar to that in a cross-flow heat recuperator. For the case with a Biot number of 0.1 or less the effectiveness of the heat and mass regenerator approaches that of a conventional recuperator with an infinite solid thermal conductivity.

The periodic steady-state performance of a cross-flow regenerator with a counter-flow arrangement for sorption is much better than that of the same regenerator with a parallel-flow arrangement. The Biot number affects the enthalpy effectiveness of a cross-flow heat and mass regenerator. For operation in the lower range of C_r/C_{min}, the lower the value of the Biot number, the higher the value of the enthalpy effectiveness. A lower value of C_r/C_{min} practically indicates a longer operating period for the switch of the adsorption and desorption modes. The value of the enthalpy effectiveness for the counterflow arrangement tends to increase as the value of C_r/C_{min} increases. Eventually it will approach to a limit and this limit is independent of the Biot number. For the parallel-flow arrangement an optimum value of C_r/C_{min} exists. The optimum C_r/C_{min} corresponds to the maximum enthalpy effectiveness for a set of Ntu, Bi and f. The maximum enthalpy effectiveness reaches a minimum for a value of Biot number near 2.0.

The value of f does not affect the value of the maximum enthalpy effectiveness. A regenerator with a higher value of f tends to require a lower value of C_r/C_{min} for its best operation. The enthalpy effectiveness increases significantly as Ntu increases. For the ideal isothermal regenerator with an infinite Ntu the enthalpy effectiveness will approach 1.0. For different outdoor air temperatures and humidity ratios the enthalpy effectiveness varies slightly. Thus, from the engineering viewpoint the enthalpy effectiveness can be considered to be independent of the outdoor climate condition.

The cross-flow heat and mass regenerator with a two-dimensional channel geometry may provide the same area density as that of a common rotary honeycomb-type heat and mass regenerator. Furthermore, the former is able to be disassembled if the structure is carefully designed. This provides an easy way to clean up the dirt trapped in the regenerator during operation. This is one of the reasons that makes the cross-flow type heat and mass regenerator an attractive device for energy recovery.

Acknowledgements—This work is supported by the Energy and Resources Laboratories at the ITRI in the Republic of China. The support and interest of Dr L. J. Fang and Dr Y. K. Chuang are greatly appreciated.

REFERENCES

1. R. V. Dunkle, A method of solar air conditioning, *Mech. Chem. Engng Trans. Inst. Engrs* **73**, 73–78 (1965).
2. I. L. Maclaine-cross, A theory of combined heat and mass transfer in regenerators, Ph.D. dissertation, Department of Mechanical Engineering, Monash University (1974).
3. I. L. Maclaine-cross and P. J. Banks, Coupled heat and mass transfer in regenerators—prediction using an analogy with heat transfer, *Int. J. Heat Mass Transfer* **15**, 1225–1242 (1972).
4. P. J. Banks, Coupled equilibrium heat and single adsorbate transfer in fluid flow through a porous medium—I. Characteristic potentials and specific capacity ratios, *Chem. Engng Sci.* **27**, 1143–1156 (1972).
5. D. J. Close and P. J. Banks, Coupled-equilibrium heat and single adsorbate transfer in fluid flow through a porous medium—II. Predictions for a silica-gel air-drier using characteristic charts, *Chem. Engng Sci.* **27**, 1157–1169 (1972).
6. P. J. Banks, Prediction of heat and mass regenerator

performance using nonlinear analogy method: part 1—basis, *J. Heat Transfer* **108,** 222–229 (1985).
7. P. J. Banks, Prediction of heat and mass regenerator performance using nonlinear analogy method: part 2—comparison of methods, *J. Heat Transfer* **107,** 230–238 (1985).
8. J. J. Jurinak, Open cycle solid desiccant cooling–component models and system simulation, Ph.D. thesis, Mechanical Engineering Department, University of Wisconsin–Madison (1982).
9. E. Van den Bulck, J. W. Mitchell and S. A. Klein, The use of dehumidifiers in desiccant cooling and dehumidification systems, *J. Heat Transfer* **108,** 684–692 (1986).
10. E. Van den Bulck, J. W. Mitchell and S. A. Klein, Design theory for rotary heat and mass exchangers—I. Wave analysis of rotary heat and mass exchangers with infinite transfer coefficients, *Int. J. Heat Mass Transfer* **28,** 1575–1586 (1985).
11. E. Van den Bulck, J. W. Mitchell and S. A. Klein, Design theory for rotary heat and mass exchangers—II. Effectiveness–number-of-transfer-units method for rotary heat and mass exchangers, *Int. J. Heat Mass Transfer* **28,** 1587–1595 (1985).
12. H. Klein, S. A. Klein and J. W. Mitchell, Analysis of regenerative enthalpy exchangers, *Int. J. Heat Mass Transfer* **33,** 735–744 (1990).
13. E. Van den Bulck and S. A. Klein, A single-blow test procedure for compact heat and mass exchangers, *J. Heat Transfer* **112,** 317–322 (1990).
14. A. A. Pesaran and A. F. Mills, Moisture transport in silica gel packed beds—I. Theoretical study, *Int. J. Heat Mass Transfer* **30,** 1037–1049 (1987).
15. A. A. Pesaran and A. F. Mills, Moisture transport in silica gel packed beds—II. Experimental study, *Int. J. Heat Mass Transfer* **30,** 1051–1060 (1987).
16. W. M. Worek and Z. Lavan, Performance of a cross-cooled desiccant dehumidifier prototype, *ASME J. Solar Energy Engng* **104,** 187–196 (1982).
17. B. Mathiprakasam and Z. Lavan, Performance predictions for adiabatic desiccant dehumidifiers using linear solutions, *ASME J. Solar Energy Engng* **102,** 73–79 (1980).
18. W. M. Kays and A. L. London, *Compact Heat Exchanger*, 3rd Edn. McGraw-Hill, New York (1984).